HAL
open science

Damage-tolerant active control using a modal H∞-norm-based methodology

Helói F.G Genari, Nazih Mechbal, Gérard Coffignal, Eurípedes G.O Nobrega

To cite this version:

Helói F.G Genari, Nazih Mechbal, Gérard Coffignal, Eurípedes G.O Nobrega. Damage-tolerant active control using a modal H∞-norm-based methodology. Control Engineering Practice, 2017, 60, pp.76-86. 10.1016/j.conengprac.2016.10.018 . hal-01493852

HAL Id: hal-01493852

https://hal.science/hal-01493852

Submitted on 29 May 2017

HAL is a multi-disciplinary open access archive for the deposit and dissemination of scientific research documents, whether they are published or not. The documents may come from teaching and research institutions in France or abroad, or from public or private research centers.

L'archive ouverte pluridisciplinaire **HAL**, est destinée au dépôt et à la diffusion de documents scientifiques de niveau recherche, publiés ou non, émanant des établissements d'enseignement et de recherche français ou étrangers, des laboratoires publics ou privés.

Damage-tolerant active control using a modal H_∞-norm-based methodology

Helói F.G. Genari[a,b,*], Nazih Mechbal[b], Gérard Coffignal[b], Eurípedes G.O. Nóbrega[a]

[a] *Department of Computational Mechanics, University of Campinas, Campinas, Brazil*
[b] *Laboratory of Process and Engineering in Mechanics and Materials, Arts et Métiers ParisTech, Paris, France*

ARTICLE INFO

Keywords:
Damage-tolerant active control
Modal H_∞ norm
Modal H_∞ control
H_∞ control
Active vibration control

ABSTRACT

A new approach for vibration reduction of flexible structures subject to damage is here proposed, based on modal H_∞-norm control. Considering that structural damage provokes different effects on each vibration mode, the proposed method concentrates the control action on modes that are indeed suffering the worst damage consequences. For this purpose, a new modal H_∞ norm is introduced, weighing each mode according to control design convenience. Based on this norm, a regular H_∞ controller design is applied, using the linear matrix inequality approach. Simulated and experimental results show significant advantages of the proposed methodology over the regular H_∞ approach, including damage tolerance.

1. Introduction

Advances in materials and associated technologies have been conducting to larger, lightweight, and more flexible structures. Consequently, these structures are more sensitive to vibrations caused by ambient disturbances, which may lead to performance worsening and eventually fatigue damage. Considering the trend of adopting light structures to nowadays engineering systems like aerospace applications, robotic systems, and communication antennae (Hu & Ng, 2005), the interest in active vibration control has been substantially increasing and several different techniques have been developed (Gu & Song, 2005; Khot, Yelve, Tomar, Desai, & Vittal, 2011; Marinaki, Marinakis, & Stavroulakis, 2010; Petersen & Pota, 2003; Zabihollah, Sedagahti, & Ganesan, 2007). However, regular active vibration control methods do not take into account the possibility of damage occurrence. To include damage compensation, guaranteeing an acceptable closed-loop performance, this paper proposes a novel modal H_∞-norm-based methodology to design damage-tolerant active controllers. Its application involves several aspects about vibration control, modal control, and fault-tolerant control, related to robustness and how to preserve performance under structural damage (Mechbal & Nóbrega, 2012).

Structural active control methods are bound to take into account a reduced order model. Continuous mechanical structures have an infinite number of vibration modes, implying that there exist always neglected dynamics in the control system design, leading to the definition of a frequency bandwidth of interest. The spillover phenomenon may be considered the main active control limitation for real applications, corresponding to the excitation of natural frequencies above this interest bandwidth. Failure in properly considering spillover in the controller design usually leads to instability (Balas, 1978, 1979; Meirovitch & Baruh, 1985; Meirovitch, Baruh, & Oz, 1983). Some proposed techniques render the problem manageable, focusing on smart structures with a great number of collocated sensors and actuators (Inman, 2001). The collocated approach corresponds to place sensors and actuators in the same location in the structure. Considering that real applications using collocated methods are not common, control technique development for noncollocated mechanical structures has been receiving the attention of the scientific community (Kim & Oh, 2013; Mechbal, Vergé, Coffignal, & Ganapathi, 2006; Schröck, Meurer, & Kugi, 2011). However, noncollocated systems have more complex dynamics with non-minimum-phase zeros, making it difficult to achieve closed-loop robustness and performance (Gosiewski & Kulesza, 2013; Mastory & Chalhoub, 2014; Preumont, 2011). Despite the progress achieved so far, the vibration control of noncollocated structures remains challenging.

Several control methods have been proposed to mitigate structure vibrations with different success levels. The spillover problem and also parameter variation are the main issues that have incurred in closed-loop instability (Bossi, Rottenbacher, Mimmi, & Magni, 2011; Mohamed, Martins, Tokhi, Sá da Costa, & Botto, 2005). However, these methods are generally inadequate to be applied to plants with dynamic uncertainties because they are very sensitive to model inaccuracy (Tang & Chen, 2009). H_∞-based control methods are able to handle both uncertainties and parameter variations, and have been successfully used to suppress low-order vibration modes (Boulet, Francis, Hughes, & Hong, 2001; Halim, 2004; Robu, Budinger,

* Corresponding author at: Department of Computational Mechanics, University of Campinas, Campinas, Brazil.
E-mail addresses: hegenari@fem.unicamp.br (H.F.G. Genari), nazih.mechbal@ensam.eu (N. Mechbal), gerard.coffignal@ensam.eu (G. Coffignal), egon@fem.unicamp.br (E.G.O. Nóbrega).

Baudouin, Prieur, & Arzelier, 2010). Due to these characteristics, the H_∞ approach has been applied to active vibration control (Nonami & Sivrioglu, 1996; Zhang, He, Wang, & Gao, 2009; Genari, Oliveira Neto, Nóbrega, Mechbal, & Coffignal, 2015). The H_∞ controller goal is to minimize the worst mode performance in the bandwidth of interest, while avoiding the excitation of the neglected dynamics. To achieve this effect, conveniently designed weighing filters are necessary to ensure the desired frequency distribution (Serpa & Nobrega, 2005). The approach generally deals with low frequency bands as a whole, which prevents mode selectivity in terms of both amplitude and frequency in the interest bandwidth. This behavior compromises the interest-bandwidth excitation as a result of the so-called water bed effect (Zhou & Doyle, 1997).

Early known papers by Balas (1978) and Meirovitch et al. (1983) introduced the modal control aiming for specific structure modes. Meirovitch developed the independent modal space control (IMSC), which changes each mode damping. However, IMSC was very sensitive with respect to spillover and improvements were proposed to make the method more tolerant to this phenomenon (Baz & Poh, 1990; Fang, Li, & Jeary, 2003; Resta, Ripamonti, Cazzulani, & Ferrari, 2010). In parallel, other modal methods have been developed (Inman, 2001; Kim, Wang, & Brennan, 2011; Pereira, Aphale, Feliu, & Moheimani, 2011). Despite the evolution, an efficient modal controller to face the spillover effects is still an open problem (Braghin, Cinquemani, & Resta, 2012; Cinquemani, Ferrari, & Bayati, 2015; Serra, Resta, & Ripamonti, 2013). A possible solution is to formulate this control system technique by merging the features of both modal and H_∞ controls. Thus, the modal selection ability of modal techniques may be incorporated with the robustness to spillover and to parametric variation of the H_∞ method.

This paper contribution is twofold: a technique for this merging approach, based on a novel modal H_∞ norm, which can be included in a regular H_∞ controller design; and the application of this control technique to achieve active damage tolerance. In addition, the proposed approach presents the capability to be applied to multiple-transducer noncollocated systems. The modal H_∞ norm conveniently weights each mode, considering the intended modes to be reduced and conducting to modal control selectivity. The problem is then solved as a classic H_∞ design, using a linear matrix inequality (LMI) approach.

Robustness and performance of the closed-loop systems are directly influenced by the accuracy of control models. However, structural dynamics are sensitive to operational conditions, temperature, and structural damage (Chomette, Rémond, Chesné, & Gaudiller, 2008; Mechbal & Nóbrega, 2015a). In most cases, the effects caused by operational condition variations can be mitigated by incorporating these changes in the controller design. On the other hand, model changes due to structural damage are not easily incorporated into the control design because damage influence in the structure dynamics is difficult to predict. Nevertheless, it is important to include the damage possibility in the structural active control design, in order to assure an acceptable performance (Genari, Mechbal, Coffignal, & Nóbrega, 2015). The structural active vibration control considering these characteristics is referred to as damage-tolerant active control (DTAC) (Mechbal & Nóbrega, 2012). DTAC is a research area derived from fault-tolerant control, focusing on the vibration control solution for mechanical structures subject to damage (Mechbal & Nóbrega, 2015b).

The objective of this paper is to propose the modal H_∞ methodology for vibration control of flexible structures and further explore its application to damaged structures. A modal method has been recently proposed to prevent fatigue damage in Chomette, Chesné, Rémond, and Gaudiller (2010). However, the goal here is more general because the modal H_∞ methodology is investigated to ensure an adequate performance before and after the damage occurrence. The proposed technique is based on the H_∞ methodology to support the parameter variations. To guarantee robustness in case of damage is not enough because robustness increase usually leads to performance loss. Thereby, the DTAC strategy here proposed aims to mitigate the damage influence in the global vibration result, while inducing a small impact on the controller performance. The proposed methodology is analyzed and compared with regular H_∞ control cases, based on experiments and simulations with different levels of complexity. For illustration purposes, a structure model using four masses connected by springs and dampers is adopted. Damage is simulated by changes in mass, stiffness, and damping coefficients. This example allows easy analysis of the modal H_∞ controller performance for DTAC applications. Then, the methodology is experimentally evaluated on two similar aluminum cantilever beams with noncollocated piezoelectric transducers. The first one is a regular beam, which is considered to be healthy, and a damage simulation is introduced into the other. A regular H_∞ controller is designed, whose performance is used as a reference. Afterward, modal controllers are designed with different modal weights in order to show the increase of the global vibration reduction. Results indicate the effectiveness of the methodology along with performance improvement compared to a regular H_∞ controller for damage tolerance.

This paper is organized as follows: in Section 2, the state-space model of a flexible structure is defined, in which the modal representation is introduced; in Section 3, the modal H_∞ norm is presented and the modal control is written as an equivalent regular H_∞ control problem; in Section 4, the validation of the modal H_∞ control methodology for regular and DTAC applications is presented, where the simulated and experimental results are analyzed; final remarks are then presented in Section 5.

2. State-space modal representation

Structure behavior is commonly represented by a second-order differential equation, which is basic to finite element modeling and can be written in the state-space representation used in the control area. Considering the nodal second-order approach, a generic flexible structure can be modeled by the following equation:

$$\mathbf{M}\ddot{\mathbf{p}}(t) + \mathbf{D}\dot{\mathbf{p}}(t) + \mathbf{K}\mathbf{p}(t) = \mathbf{B}_0\mathbf{f}(t), \tag{1}$$

in which $\mathbf{p}(t)$ denotes the displacements, $\mathbf{M}$ is the mass matrix, $\mathbf{D}$ is the damping matrix, $\mathbf{K}$ is the stiffness matrix, $\mathbf{B}_0$ denotes the input matrix, and $\mathbf{f}(t)$ represents the external forces acting on the structure. Usually, the flexible structure models have a large order and this complicates the dynamic analysis due to numerical difficulties and high computational costs. Thus, it is convenient to write an equivalent system with a proper number of modes. The modal coordinates are often used in the dynamic analysis to reduce the model order. Assuming that m is the number of selected modes, the modal matrix is defined as:

$$\mathbf{\Phi} = [\boldsymbol{\phi}_1 \;\; \boldsymbol{\phi}_2 \;\; \cdots \;\; \boldsymbol{\phi}_\mathbf{m}].$$

Considering a coordinate transformation given by $\mathbf{p}(t) = \mathbf{\Phi}\mathbf{q}(t)$, and pre-multiplying (1) by $\mathbf{\Phi}^T$:

$$\begin{aligned}&\mathbf{\Phi}^T\mathbf{M}\mathbf{\Phi}\ddot{\mathbf{q}}(t) + \mathbf{\Phi}^T\mathbf{D}\mathbf{\Phi}\dot{\mathbf{q}}(t) + \mathbf{\Phi}^T\mathbf{K}\mathbf{\Phi}\mathbf{q}(t) = \mathbf{\Phi}^T\mathbf{B}_0\mathbf{f}(t)\\ &\mathbf{M}_\mathbf{m}\ddot{\mathbf{q}}(t) + \mathbf{D}_\mathbf{m}\dot{\mathbf{q}}(t) + \mathbf{K}_\mathbf{m}\mathbf{q}(t) = \mathbf{\Phi}^T\mathbf{B}_0\mathbf{f}(t),\end{aligned} \tag{2}$$

in which $\mathbf{M}_\mathbf{m} = \mathbf{\Phi}^T\mathbf{M}\mathbf{\Phi}$, $\mathbf{D}_\mathbf{m} = \mathbf{\Phi}^T\mathbf{D}\mathbf{\Phi}$, and $\mathbf{K}_\mathbf{m} = \mathbf{\Phi}^T\mathbf{K}\mathbf{\Phi}$. While matrices $\mathbf{M}_\mathbf{m}$ and $\mathbf{K}_\mathbf{m}$ are diagonal, $\mathbf{D}_\mathbf{m}$ is not always diagonal. For analytical convenience, the damping matrix is considered as a linear combination of stiffness and mass matrices, $\mathbf{D} = \alpha\mathbf{M} + \beta\mathbf{K}$. In general, this approach is justified by the fact that flexible structures have very small damping factors.

Pre-multiplying (2) by $\mathbf{M}_\mathbf{m}^{-1}$, which is assumed nonsingular, it results in

$$\ddot{\mathbf{q}}(t) + \mathbf{M}_\mathbf{m}^{-1}\mathbf{D}_\mathbf{m}\dot{\mathbf{q}}(t) + \mathbf{M}_\mathbf{m}^{-1}\mathbf{K}_\mathbf{m}\mathbf{q}(t) = \mathbf{M}_\mathbf{m}^{-1}\mathbf{\Phi}^T\mathbf{B}_0\mathbf{f}(t)$$

and equivalently:

$$\ddot{\mathbf{q}}(t) + 2\mathbf{Z}\mathbf{\Omega}\dot{\mathbf{q}}(t) + \mathbf{\Omega}^2\mathbf{q}(t) = \mathbf{B}_\mathbf{m}\mathbf{f}(t), \tag{3}$$

in which $\mathbf{\Omega}^2 = \mathbf{M_m^{-1}K_m}$, $\mathbf{Z} = 0.5\mathbf{M_m^{-1}D_m\Omega^{-1}}$, $\mathbf{B_m} = \mathbf{M_m^{-1}\Phi^T B_0}$, and $\mathbf{q}(t)$ represents the modal displacement vector.

Eq. (3), a structure modal representation, is a set of uncoupled second-order differential equations and can be written as a set of m independent equations:

$$\ddot{q}_i(t) + 2\xi_i\omega_i\dot{q}_i(t) + \omega_i^2 q_i(t) = \mathbf{b_{mi}f}(t), \quad i = 1,\ldots,m, \tag{4}$$

in which ω_i and ξ_i are respectively the natural frequency and the damping factor of mode i.

From (4), it is easy to express the set of second-order differential equations as a state-space modal equation:

$$\dot{\mathbf{x}}(t) = \mathbf{Ax}(t) + \mathbf{Bf}(t), \tag{5}$$

where $\mathbf{x}(t)$ represents the state vector, $\mathbf{B}$ is a modal input matrix, and $\mathbf{A}$ is a block-diagonal matrix. The state variable definition conducts to a specific modal model, of which some examples are given in Gawronski (2004). However, for all these canonical models, $\mathbf{A}$ and $\mathbf{B}$ have the following representation:

$$\mathbf{A} = \begin{bmatrix} \mathbf{A}_1 & \mathbf{0} & \cdots & \mathbf{0} \\ \mathbf{0} & \mathbf{A}_2 & \cdots & \mathbf{0} \\ \vdots & \vdots & \ddots & \vdots \\ \mathbf{0} & \mathbf{0} & \cdots & \mathbf{A_m} \end{bmatrix} \quad \text{and} \quad \mathbf{B} = \begin{bmatrix} \mathbf{b}_1 \\ \mathbf{b}_2 \\ \vdots \\ \mathbf{b_m} \end{bmatrix},$$

where $\mathbf{A}_i$ is a 2×2 matrix for $i = 1\ldots m$, therefore isolating each mode.

3. Modal robust control

The next subsections present the modal H_∞ control technique details. Initially, the modal H_∞ norm is defined from the $\mathcal{L}_2$-induced norm. Then, the modal H_∞ problem is formulated as a regular H_∞ problem. Finally, the last subsection shows that the modal robust controller design can be formulated as a convex programming problem, based on an LMI approach.

3.1. Modal norm definition

This subsection introduces the modal H_∞ norm. Initially, the relation between the H_∞ norm of a linear time-invariant system and the respective modal behavior is presented. Then, the involved concepts are used to propose the modal H_∞ norm.

Consider a stable linear time-invariant system with distinct natural frequencies represented by the transfer matrix $G(s)$, where s is the Laplace variable. Assuming a disturbance $W(s)$ such that $\mathbf{w}(t) \in \mathcal{L}_2$, the respective system output is given by $Y(s) = G(s)W(s)$. Dividing the system frequency response into m bands, with only one mode in each band, this leads to

$$Y(s) = \sum_{i=1}^{m} \widetilde{Y}_i(s) = \sum_{i=1}^{m} G(s)W_i(s) = \sum_{i=1}^{m} G(s)F_i[W(s)], \tag{6}$$

where F_i is an ideal bandpass filter and $W_i(s)$ is the disturbance at band i.

The induced H_∞ norm of $G(s)$ may be written as:

$$\| G(s)\|_\infty^2 = \underbrace{\sup}_{\mathbf{w}\neq 0,\ \mathbf{w}\in\mathcal{L}_2[0,\infty)} \frac{\int_0^\infty \mathbf{y}^T(t)\mathbf{y}(t)dt}{\int_0^\infty \mathbf{w}^T(t)\mathbf{w}(t)dt}, \tag{7}$$

where $\mathbf{y}(t)$ and $\mathbf{w}(t)$ are respectively the output and the input of $G(s)$ in the time domain. Eq. (7) may be written as:

$$\| G(s)\|_\infty^2 = \underbrace{\sup}_{\mathbf{w}\neq 0,\ \mathbf{w}\in\mathcal{L}_2[0,\infty)} \frac{\int_0^\infty (\sum_{i=1}^m \widetilde{\mathbf{y}}_i(t))^T(\sum_{j=1}^m \widetilde{\mathbf{y}}_j(t))dt}{\int_0^\infty (\sum_{i=1}^m \mathbf{w}_i(t))^T(\sum_{j=1}^m \mathbf{w}_j(t))dt}.$$

Or, introducing $\boldsymbol{\delta}_{\tilde{\mathbf{y}}}$ and $\boldsymbol{\delta}_{\mathbf{w}}$ to represent the cross terms for $i \neq j$, it leads to

$$\| G(s)\|_\infty^2 = \underbrace{\sup}_{\mathbf{w}\neq 0,\ \mathbf{w}\in\mathcal{L}_2[0,\infty)} \frac{\int_0^\infty (\sum_{i=1}^m \widetilde{\mathbf{y}}_i^T(t)\widetilde{\mathbf{y}}_i(t) + \boldsymbol{\delta}_{\tilde{\mathbf{y}}})dt}{\int_0^\infty (\sum_{i=1}^m \mathbf{w}_i^T(t)\mathbf{w}_i(t) + \boldsymbol{\delta}_{\mathbf{w}})dt}.$$

The following theorem has the objective of proving that the contribution of these cross terms can be disregarded, aiming for a system representation that is more suitable to achieve an H_∞ controller design.

Theorem 1. *Given a scalar $\gamma > 0$ and a stable linear time-invariant system with distinct natural frequencies represented by the transfer matrix $G(s)$, where the output signal vector $\mathbf{y}(t)$ is decomposed into m frequency bands according to (6), if*

$$\underbrace{\sup}_{\mathbf{w}\neq 0,\ \mathbf{w}\in\mathcal{L}_2[0,\infty)} \frac{\int_0^\infty \mathbf{y}^T(t)\mathbf{y}(t)dt}{\int_0^\infty \mathbf{w}^T(t)\mathbf{w}(t)dt} < \gamma^2,$$

then

$$\underbrace{\sup}_{\mathbf{w}\neq 0,\ \mathbf{w}\in\mathcal{L}_2[0,\infty)} \frac{\sum_{i=1}^m \int_0^\infty \widetilde{\mathbf{y}}_i^T(t)\widetilde{\mathbf{y}}_i(t)dt}{\sum_{i=1}^m \int_0^\infty \mathbf{w}_i^T(t)\mathbf{w}_i(t)dt} < \gamma^2.$$

Proof. The H_∞-norm definition (7) bounded by the scalar γ may be written as:

$$\| G(s)\|_\infty^2 = \underbrace{\sup}_{\mathbf{w}\neq 0,\ \mathbf{w}\in\mathcal{L}_2[0,\infty)} \frac{\int_0^\infty \mathbf{y}^T(t)\mathbf{y}(t)dt}{\int_0^\infty \mathbf{w}^T(t)\mathbf{w}(t)dt} < \gamma^2.$$

Considering the Parseval's theorem, it is possible to write the following expression:

$$\begin{aligned}
\sum_{i=1}^m \int_0^\infty \widetilde{\mathbf{y}}_i^T(t)\widetilde{\mathbf{y}}_i(t)dt &= \frac{1}{2\pi}\sum_{i=1}^m \int_{-\infty}^\infty \widetilde{Y}_i^*(j\omega)\widetilde{Y}_i(j\omega)d\omega \\
&= \frac{1}{2\pi}\sum_{i=1}^m \int_{-\infty}^\infty W_i^*(j\omega)G^*(j\omega)G(j\omega)W_i(j\omega)d\omega \\
&\leq \| G(s)\|_\infty^2 \frac{1}{2\pi}\sum_{i=1}^m \int_{-\infty}^\infty W_i^*(j\omega)W_i(j\omega)d\omega \\
&\leq \| G(s)\|_\infty^2 \sum_{i=1}^m \int_0^\infty \mathbf{w}_i^T(t)\mathbf{w}_i(t)dt.
\end{aligned}$$

This leads to

$$\| G(s)\|_\infty^2 \geq \underbrace{\sup}_{\mathbf{w}\neq 0,\ \mathbf{w}\in\mathcal{L}_2[0,\infty)} \frac{\sum_{i=1}^m \int_0^\infty \widetilde{\mathbf{y}}_i^T(t)\widetilde{\mathbf{y}}_i(t)dt}{\sum_{i=1}^m \int_0^\infty \mathbf{w}_i^T(t)\mathbf{w}_i(t)dt}.$$

Considering that $\| G(s)\|_\infty^2 < \gamma^2$, it is possible to conclude that

$$\underbrace{\sup}_{\mathbf{w}\neq 0,\ \mathbf{w}\in\mathcal{L}_2[0,\infty)} \frac{\sum_{i=1}^m \int_0^\infty \widetilde{\mathbf{y}}_i^T(t)\widetilde{\mathbf{y}}_i(t)dt}{\sum_{i=1}^m \int_0^\infty \mathbf{w}_i^T(t)\mathbf{w}_i(t)dt} < \gamma^2.$$

This proves the theorem. □

Theorem 1 relates the H_∞ norm to a truncated decomposition of the linear system as a summation of bandpass components. Applying the modal expansion theorem (Inman, 1989), the system output may be decomposed into a summation of modal responses such that

$$Y(s) = \sum_{i=1}^m \overline{Y}_i(s) = \sum_{i=1}^m G_i(s)W(s),$$

where $G_i(s)$ is the mode i submatrix that composes $G(s)$.

The output $\widetilde{Y}_i(s)$ is the system response due to all modes in the region of the mode i and $\overline{Y}_i(s)$ corresponds to the response of only mode

i in the same region. For each frequency band, the main contribution to the amplitude of $\widetilde{Y}_i(s)$ is due to the amplitude of the resonant frequency response in the band, with the addition of all the other mode responses in the same band (Gawronski, 2008). Taking into account that the H_∞ norm is an intrinsic characteristic of the system, it does not depend on the excitation. In particular, the response to the summation of the modal excitations is bounded by the H_∞ norm (Gawronski, 2004). So, it may be written that

$$\underbrace{\sup}_{\mathbf{w}\neq 0,\ \mathbf{w}\in\mathcal{L}_2[0,\infty)} \frac{\sum_{i=1}^{m}\int_0^\infty \overline{\mathbf{y}}_i^T(t)\overline{\mathbf{y}}_i(t)dt}{\sum_{i=1}^{m}\int_0^\infty \mathbf{w}_i^T(t)\mathbf{w}_i(t)dt} < \gamma^2. \tag{8}$$

Based on (8), it is possible to define a weighted norm to balance the contribution of each mode.

Proposition 1. *The weighted modal H_∞ norm of a stable linear time-invariant system $G(s)$ with distinct natural frequencies is proposed as*:

$$\begin{aligned}\| G(s)\|_{\infty,\mathbf{Q}}^2 &= \underbrace{\sup}_{\mathbf{w}\neq 0,\ \mathbf{w}\in\mathcal{L}_2[0,\infty)} \frac{\sum_{i=1}^{m}\int_0^\infty \overline{\mathbf{y}}_i^T(t)\mathbf{Q}_i\overline{\mathbf{y}}_i(t)dt}{\sum_{i=1}^{m}\int_0^\infty \mathbf{w}_i^T(t)\mathbf{w}_i(t)dt}\\ &= \underbrace{\sup}_{\mathbf{w}\neq 0,\ \mathbf{w}\in\mathcal{L}_2[0,\infty)} \frac{\int_0^\infty \hat{\mathbf{y}}^T(t)\mathbf{Q}\hat{\mathbf{y}}(t)dt}{\int_0^\infty \widehat{\mathbf{w}}^T(t)\widehat{\mathbf{w}}(t)dt} = \underbrace{\sup}_{\mathbf{w}\neq 0,\ \mathbf{w}\in\mathcal{L}_2[0,\infty)} \frac{\| \hat{\mathbf{y}}(t)\|_{2,\mathbf{Q}}^2}{\| \widehat{\mathbf{w}}(t)\|_2^2},\end{aligned}$$

in which $\hat{\mathbf{y}}^T(t) = [\overline{\mathbf{y}}_1^T(t)\ \overline{\mathbf{y}}_2^T(t)\cdots\overline{\mathbf{y}}_m^T(t)]$, $\widehat{\mathbf{w}}^T(t) = [\mathbf{w}_1^T(t)\ \mathbf{w}_2^T(t)\cdots\mathbf{w}_m^T(t)]$, $\mathbf{Q}_i > 0$ *is a diagonal matrix, and* $\mathbf{Q} = \mathrm{diag}(\mathbf{Q}_1, \mathbf{Q}_2, \ldots, \mathbf{Q}_m)$.

3.2. Modal control problem

The following plant in the state-space representation is generally adopted to design the H_∞ controllers:

$$\begin{aligned}\dot{\mathbf{x}}(t) &= \mathbf{A}\mathbf{x}(t) + \mathbf{B}_1\mathbf{w}(t) + \mathbf{B}_2\mathbf{u}(t)\\ \mathbf{z}(t) &= \mathbf{C}_1\mathbf{x}(t) + \mathbf{D}_{11}\mathbf{w}(t) + \mathbf{D}_{12}\mathbf{u}(t)\\ \mathbf{y}(t) &= \mathbf{C}_2\mathbf{x}(t) + \mathbf{D}_{21}\mathbf{w}(t) + \mathbf{D}_{22}\mathbf{u}(t),\end{aligned} \tag{9}$$

in which $\mathbf{y}(t)$ is the output vector, $\mathbf{u}(t)$ represents the control signal vector, $\mathbf{w}(t)$ is the disturbance vector, and $\mathbf{z}(t)$ is the performance vector chosen by the controller design; $\mathbf{A}$ is the system matrix, $\mathbf{B} = [\mathbf{B}_1\ \mathbf{B}_2]$ is the input matrix, and matrices $\mathbf{C}$s and $\mathbf{D}$s balance the state vector and input signals to create $\mathbf{y}(t)$ and $\mathbf{z}(t)$. All vectors and matrices have appropriate dimensions related to the number of inputs and outputs and to the model order.

The H_∞ control problem is to find a controller K_c to the plant (9), if there is one, stated as:

$$\begin{aligned}\dot{\mathbf{x}}_c(t) &= \mathbf{A}_c\mathbf{x}_c(t) + \mathbf{B}_c\mathbf{y}(t)\\ \mathbf{u}(t) &= \mathbf{C}_c\mathbf{x}_c(t) + \mathbf{D}_c\mathbf{y}(t)\end{aligned} \tag{10}$$

such that, for the closed-loop system and given a $\gamma > 0$,

$$\underbrace{\inf}_{K_c\in V}\ \underbrace{\sup}_{\mathbf{w}\neq 0,\ \mathbf{w}\in\mathcal{L}_2[0,\infty)} \frac{\int_0^\infty \mathbf{z}^T(t)\mathbf{z}(t)dt}{\int_0^\infty \mathbf{w}^T(t)\mathbf{w}(t)dt} < \gamma^2,$$

in which V represents the set of all controllers that stabilizes the plant.

Defining a new modal performance output, the following theorem provides conditions to transform the modal H_∞ problem into a regular H_∞ problem.

Theorem 2 (*Modal H_∞ theorem*). *Consider the H_∞ problem of designing a controller K_c (10) for a structure according to (9) with the modal state matrix according to (5) and the following performance output*:

$$\mathbf{z}_\mathbf{p}(t) = \mathbf{\Gamma}\mathbf{x}(t) + \mathbf{\Theta}\mathbf{w}(t) + \mathbf{\Lambda}\mathbf{u}(t),$$

with

$$\mathbf{\Gamma} = \begin{bmatrix}\mathbf{Q}_1^{\frac{1}{2}}\mathbf{C}_{1_1} & \mathbf{Q}_2^{\frac{1}{2}}\mathbf{C}_{1_2} & \cdots & \mathbf{Q}_m^{\frac{1}{2}}\mathbf{C}_{1_m}\end{bmatrix},\ \mathbf{\Theta} = (\mathbf{Q}_1^{\frac{1}{2}}\mathbf{D}_{11_1}+\cdots+\mathbf{Q}_m^{\frac{1}{2}}\mathbf{D}_{11_m}),$$

$$\mathbf{\Lambda} = (\mathbf{Q}_1^{\frac{1}{2}}\mathbf{D}_{12_1}+\cdots+\mathbf{Q}_m^{\frac{1}{2}}\mathbf{D}_{12_m}),$$

where the diagonal matrix $\mathbf{Q}_i > 0$ weights mode i and $\mathbf{C}_{1_i}$, $\mathbf{D}_{11_i}$, and $\mathbf{D}_{12_i}$ correspond to the respective mode i submatrices in $\mathbf{C}_1$, $\mathbf{D}_{11}$, and *$\mathbf{D}_{12}$.Then, given a scalar $\gamma > 0$, a controller that solves the respective H_∞ problem,*

$$\| T_{\mathbf{z}_\mathbf{p}\mathbf{w}}(s)\|_\infty < \gamma,$$

also guarantees that

$$\| T_{\mathbf{z}\mathbf{w}}(s)\|_{\infty,\mathbf{Q}} < \gamma,$$

where $T_{\mathbf{z}_\mathbf{p}\mathbf{w}}(s)$ and $T_{\mathbf{z}\mathbf{w}}(s)$ are the closed-loop transfer matrices using K_c for the modal performance vectors.

Proof. Solving the respective H_∞ problem implies that

$$\underbrace{\sup}_{\mathbf{w}\neq 0,\ \mathbf{w}\in\mathcal{L}_2[0,\infty)} \frac{\int_0^\infty \mathbf{z}_\mathbf{p}^T(t)\mathbf{z}_\mathbf{p}(t)dt}{\int_0^\infty \mathbf{w}^T(t)\mathbf{w}(t)dt} < \gamma^2.$$

Considering the decomposition of $\mathbf{z}_\mathbf{p}(t)$ into modal components such as $\mathbf{z}_\mathbf{p}(t) = \sum_{i=1}^{m}\mathbf{z}_{\mathbf{p}_i}(t)$ for $i = 1\ldots m$, then $\mathbf{z}_{\mathbf{p}_i}(t)$ can be defined as:

$$\mathbf{z}_{\mathbf{p}_i}(t) = \mathbf{\Gamma}_i\mathbf{X}_i(t) + \mathbf{\Theta}_i\mathbf{w}(t) + \mathbf{\Lambda}_i\mathbf{u}(t),$$

in which $\mathbf{X}_i(t)$ represents the state vector of mode i and $\mathbf{\Gamma}_i$, $\mathbf{\Theta}_i$, and $\mathbf{\Lambda}_i$ are respectively the submatrix of $\mathbf{\Gamma}$, $\mathbf{\Theta}$, and $\mathbf{\Lambda}$ relative to mode i.

Writing $\mathbf{\Gamma}_i$, $\mathbf{\Theta}_i$, and $\mathbf{\Lambda}_i$ as:

$$\mathbf{\Gamma}_i = \mathbf{Q}_i^{\frac{1}{2}}\mathbf{C}_{1_i},\ \mathbf{\Theta}_i = \mathbf{Q}_i^{\frac{1}{2}}\mathbf{D}_{11_i},\ \mathbf{\Lambda}_i = \mathbf{Q}_i^{\frac{1}{2}}\mathbf{D}_{12_i},$$

where $\mathbf{C}_{1_i}$, $\mathbf{D}_{11_i}$, and $\mathbf{D}_{12_i}$ are the modal submatrices relative to mode i of the performance vector based on $\mathbf{z}(t)$ according to (9). The modal submatrices can be used to reconstruct the full modal performance vector as:

$$\begin{aligned}\mathbf{z}_\mathbf{p}(t) &= \sum_{i=1}^{m}(\mathbf{\Gamma}_i\mathbf{X}_i(t) + \mathbf{\Theta}_i\mathbf{w}(t) + \mathbf{\Lambda}_i\mathbf{u}(t))\\ &= \begin{bmatrix}\mathbf{Q}_1^{\frac{1}{2}}\mathbf{C}_{1_1} & \mathbf{Q}_2^{\frac{1}{2}}\mathbf{C}_{1_2} & \cdots & \mathbf{Q}_m^{\frac{1}{2}}\mathbf{C}_{1_m}\end{bmatrix}\mathbf{x}(t) + (\mathbf{Q}_1^{\frac{1}{2}}\mathbf{D}_{11_1}+\cdots+\mathbf{Q}_m^{\frac{1}{2}}\mathbf{D}_{11_m})\mathbf{w}(t)\\ &\quad + (\mathbf{Q}_1^{\frac{1}{2}}\mathbf{D}_{12_1}+\cdots+\mathbf{Q}_m^{\frac{1}{2}}\mathbf{D}_{12_m})\mathbf{u}(t).\end{aligned}$$

Consequently, the product $\mathbf{z}_{\mathbf{p}_i}^T(t)\mathbf{z}_{\mathbf{p}_i}(t)$ is given by:

$$\mathbf{z}_{\mathbf{p}_i}^T(t)\mathbf{z}_{\mathbf{p}_i}(t) = [\mathbf{X}_i^T(t)\ \ \mathbf{w}^T(t)\ \ \mathbf{u}^T(t)]\begin{bmatrix}\mathbf{C}_{1_i}^T\\ \mathbf{D}_{11_i}^T\\ \mathbf{D}_{12_i}^T\end{bmatrix}\mathbf{Q}_i[\mathbf{C}_{1_i}\ \ \mathbf{D}_{11_i}\ \ \mathbf{D}_{12_i}]\begin{bmatrix}\mathbf{X}_i(t)\\ \mathbf{w}(t)\\ \mathbf{u}(t)\end{bmatrix},$$

which leads to

$$\mathbf{z}_{\mathbf{p}_i}^T(t)\mathbf{z}_{\mathbf{p}_i}(t) = \mathbf{z}_i^T(t)\mathbf{Q}_i\mathbf{z}_i(t). \tag{11}$$

Based on Theorem 1 and statement (11), it follows:

$$\underbrace{\sup}_{\mathbf{w}\neq 0,\ \mathbf{w}\in\mathcal{L}_2[0,\infty)} \frac{\sum_{i=1}^{m}\int_0^\infty \mathbf{z}_{\mathbf{p}_i}^T(t)\mathbf{z}_{\mathbf{p}_i}(t)dt}{\sum_{i=1}^{m}\int_0^\infty \mathbf{w}_i^T(t)\mathbf{w}_i(t)dt} = \underbrace{\sup}_{\mathbf{w}\neq 0,\mathbf{w}\in\mathcal{L}_2[0,\infty)} \frac{\sum_{i=1}^{m}\int_0^\infty \mathbf{z}_i^T(t)\mathbf{Q}_i\mathbf{z}_i(t)dt}{\sum_{i=1}^{m}\int_0^\infty \mathbf{w}_i^T(t)\mathbf{w}_i(t)dt} < \gamma^2,$$

which comes to

$$\| T_{\mathbf{z}\mathbf{w}}(s)\|_{\infty,\mathbf{Q}} < \gamma.$$

This proves the theorem.□

The proposed modal H_∞ technique allows that the control system designer prioritizes a specific mode vibration reduction by changing only its respective weighing matrix. For instance, when a structure is submitted to severe stress conditions due to external excitation of a mode. The excitation persistency may affect the structure lifetime,

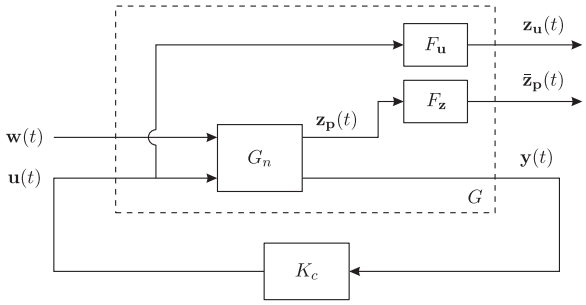

Fig. 1. Block diagram of the H_∞ control problem.

potentially causing damage that may result in vibration increase. This cycle may contribute to damage severity increase, leading to undesirable consequences such as catastrophic failure. Thus, an adequate modal control is needed to mitigate this undesired cycle.

3.3. Modal control solution

It was shown that the modal control solution is obtained using the regular H_∞ approach (Gahinet, Nemirovski, Laub, & Chilali, 1995; Gawronski, 2004; Zhou & Doyle, 1997). Usually, the H_∞ controllers are computed using two different methodologies: Riccati equations and LMIs. The LMI approach has the advantage that it is possible to include additional restriction equations into the problem and that the final minimization problem keeps its convexity, permitting to be solved by efficient interior-point methods (Chilali & Gahinet, 1996; Nesterov & Nemirovski, 1994).

The H_∞ control problem can be summarized in the block diagram of Fig. 1. In this figure, the filters $F_{\mathbf{u}}$ and $F_{\mathbf{z}}$ are applied to the control signal vector $\mathbf{u}(t)$ and the performance vector $\mathbf{z_p}(t)$, generating respectively $\mathbf{z_u}(t)$ and $\bar{\mathbf{z}}_{\mathbf{p}}(t)$. The disturbance forces are represented by $\mathbf{w}(t)$ and the output vector is $\mathbf{y}(t)$. The nominal plant is denoted by G_n, the generalized plant, by G_p, and the nominal controller is K_c.

The weighing filters are key elements in the controller design process and often involve many iterations and fine tuning. To obtain a good trade-off between performance and robustness, $F_{\mathbf{z}}(s)$ is designed as a low-pass weighing filter. To avoid spillover phenomenon, $F_{\mathbf{u}}(s)$ is designed as a high-pass weighing filter. In general, the weighing filters are designed as (Zhou & Doyle, 1997):

$$F_{\mathbf{z}}(s) = \left(\frac{\dfrac{s}{\sqrt[k]{M}} + \omega_c}{s + \omega_c \sqrt[k]{\varepsilon}}\right)^k \quad \text{and} \quad F_{\mathbf{u}}(s) = \left(\frac{s + \dfrac{\omega_c}{\sqrt[k]{M}}}{s\sqrt[k]{\varepsilon} + \omega_c}\right)^k, \tag{12}$$

in which ω_c, k, ε, and M determine the transition frequency between rejection band and passband, the filter order, the gain at passband, and the gain at rejection band, respectively.

The H_∞ norm of the transfer function between the disturbance $\mathbf{w}(t)$ and the performance output $\hat{\mathbf{z}}(t) = [\bar{\mathbf{z}}_{\mathbf{p}}^T(t)\ \mathbf{z}_{\mathbf{u}}^T(t)]^T$ is designated by $\|T_{\hat{\mathbf{z}}\mathbf{w}}\|_\infty$. Thus, the H_∞ controller design consists in finding a central controller K_c that minimizes $\|T_{\hat{\mathbf{z}}\mathbf{w}}\|_\infty$. It is usual to solve a suboptimal problem that minimizes $\|T_{\hat{\mathbf{z}}\mathbf{w}}\|_\infty$ through iterations, as presented in Section 3.2. Therefore, the robust controller design can be formulated as a convex programming problem, adopting a well-known procedure presented in Gahinet and Apkarian (1994) and Gahinet et al. (1995).

4. Simulated and experimental results

This section presents experimental and analytical results concerning DTAC. Initially, the modal H_∞ control methodology is examined in a simple structure with four masses connected by springs and dampers, and damage is simulated through changes in these parameters. This structure is used to examine the proposed technique for different damage locations and severities. After that, the methodology is experimentally tested using two similar aluminum beams, one integer and the second with a simulated damage, both with cantilever boundary conditions and noncollocated piezoelectric transducers.

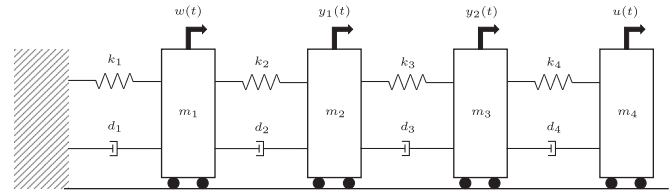

Fig. 2. Simulated structure.

4.1. Simulated structure results

The simulated structure is presented in Fig. 2. This example is used for illustration purposes, allowing easy reproducibility and easy DTAC application analysis. Masses, stiffness, and damping coefficients are represented respectively by m_e, k_e, and d_e for $e = 1,\ldots,4$. The signal $w(t)$ represents the disturbance signal acting on mass m_1, and $u(t)$ is the control signal acting on mass m_4. The outputs $y_1(t)$ and $y_2(t)$ are the displacements of masses m_2 and m_3, respectively.

This simple structure can be modeled by (1):

$$\mathbf{M}\ddot{\mathbf{p}}(t) + \mathbf{D}\dot{\mathbf{p}}(t) + \mathbf{K}\mathbf{p}(t) = \underbrace{[\widetilde{\mathbf{B}}_1\ \widetilde{\mathbf{B}}_2]}_{\mathbf{B}_0}\underbrace{\begin{bmatrix} w(t) \\ u(t) \end{bmatrix}}_{\mathbf{f}(t)},$$

where

$$\mathbf{M} = \begin{bmatrix} m_1 & 0 & 0 & 0 \\ 0 & m_2 & 0 & 0 \\ 0 & 0 & m_3 & 0 \\ 0 & 0 & 0 & m_4 \end{bmatrix}, \quad \mathbf{D} = \begin{bmatrix} d_1 + d_2 & -d_2 & 0 & 0 \\ -d_2 & d_2 + d_3 & -d_3 & 0 \\ 0 & -d_3 & d_3 + d_4 & -d_4 \\ 0 & 0 & -d_4 & d_4 \end{bmatrix},$$

$$\widetilde{\mathbf{B}}_1 = \begin{bmatrix} 1 \\ 0 \\ 0 \\ 0 \end{bmatrix}, \mathbf{K} = \begin{bmatrix} k_1 + k_2 & -k_2 & 0 & 0 \\ -k_2 & k_2 + k_3 & -k_3 & 0 \\ 0 & -k_3 & k_3 + k_4 & -k_4 \\ 0 & 0 & -k_4 & k_4 \end{bmatrix}, \quad \text{and} \quad \widetilde{\mathbf{B}}_2 = \begin{bmatrix} 0 \\ 0 \\ 0 \\ 1 \end{bmatrix}.$$

The control objective is to reduce the vibration of masses m_2 and m_3 due to disturbance $w(t)$ on mass m_1. Thus, to design the regular H_∞ controller, it is necessary to transform the model into the state-space form:

$$\overline{\mathbf{A}} = \begin{bmatrix} \mathbf{0} & \mathbf{I} \\ -\mathbf{M}^{-1}\mathbf{K} & -\mathbf{M}^{-1}\mathbf{D} \end{bmatrix}, \quad \overline{\mathbf{B}}_1 = \begin{bmatrix} \mathbf{0} \\ \mathbf{M}^{-1}\widetilde{\mathbf{B}}_1 \end{bmatrix},$$

$$\overline{\mathbf{B}}_2 = \begin{bmatrix} \mathbf{0} \\ \mathbf{M}^{-1}\widetilde{\mathbf{B}}_2 \end{bmatrix}, \overline{\mathbf{C}}_1 = \begin{bmatrix} 0 & 1 & 0 & 0 & 0 & 0 & 0 & 0 \\ 0 & 0 & 1 & 0 & 0 & 0 & 0 & 0 \end{bmatrix}, \quad \overline{\mathbf{C}}_1 = \overline{\mathbf{C}}_2,$$

$$\text{and} \quad \overline{\mathbf{D}}_{11} = \overline{\mathbf{D}}_{12} = \overline{\mathbf{D}}_{21} = \overline{\mathbf{D}}_{22} = \begin{bmatrix} 0 \\ 0 \end{bmatrix}.$$

To simulate this simple structure, mass and stiffness values are selected as $m_1 = 3$ kg, $m_2 = 2$ kg, $m_3 = 2$ kg, $m_4 = 3$ kg, $k_1 = 4800$ N/m, $k_2 = 2200$ N/m, $k_3 = 1200$ N/m, and $k_4 = 500$ N/m. The proportional damping matrix is adopted according to: $\mathbf{D} = 0.0005\mathbf{K} + 0.001\mathbf{M}$. The modal model (9) is obtained using the function *canon* and the H_∞ controllers are designed using *mincx*, both functions of MATLAB®. The open-loop and closed-loop results are shown in Fig. 3. The regular H_∞ controller (RC) reduces peak vibration in the four modes, but it is still possible to increase performance by using the modal H_∞ controller (MC). Analyzing T_{z_1w} presented in Fig. 3a, the greatest reduction corresponds to the first mode. Thus, to increase control performance, modes 2, 3, and 4 should be weighted, focusing on modes 3 and 4 due to the small vibration reduction using the RC. The weights for modes 1, 2, 3, and 4 are chosen as 0.6, 1.3, 1.6, and 1.6, respectively. The RC performance for T_{z_2w} is similar to T_{z_1w}. However, the vibration reduction should be increased in modes 2 and 3 because the mode 4 has a small

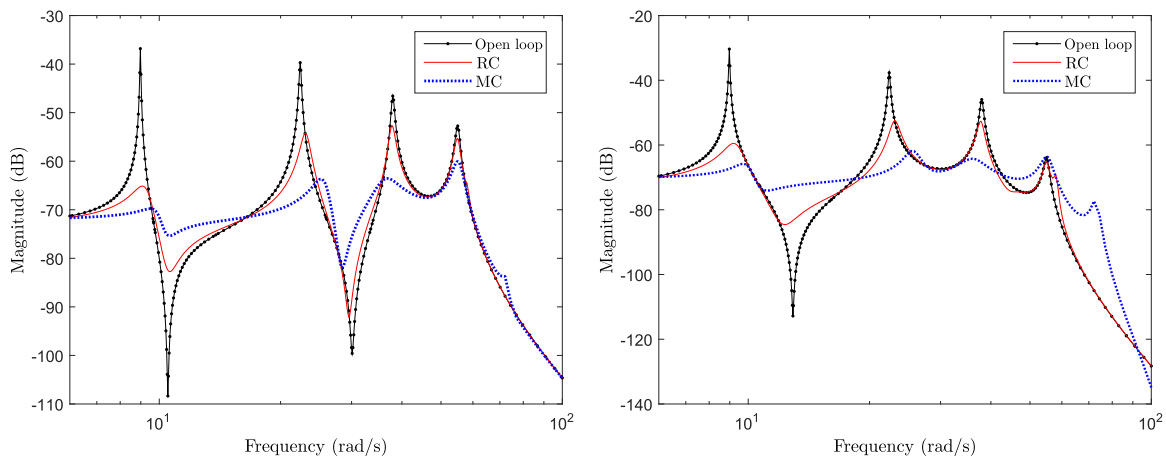

(a) $T_{z_1 w}$. (b) $T_{z_2 w}$.

Fig. 3. Simulated results of the healthy structure.

magnitude, as can be seen in Fig. 3b. For $T_{z_2 w}$, the weights are respectively 1, 1.6, 1.4, and 0.6 for modes 1, 2, 3, and 4. Thereby, the weighing matrices are depicted as:

$$\mathbf{Q_1^{\frac{1}{2}}} = \begin{bmatrix} 0.6 & 0 \\ 0 & 1 \end{bmatrix}, \quad \mathbf{Q_2^{\frac{1}{2}}} = \begin{bmatrix} 1.3 & 0 \\ 0 & 1.6 \end{bmatrix}, \quad \mathbf{Q_3^{\frac{1}{2}}} = \begin{bmatrix} 1.6 & 0 \\ 0 & 1.4 \end{bmatrix},$$

and $\mathbf{Q_4^{\frac{1}{2}}} = \begin{bmatrix} 1.6 & 0 \\ 0 & 0.6 \end{bmatrix}$.

Fig. 3 presents the comparison between the open-loop and closed-loop systems, demonstrating the performance increase in the weighted modes. To test the effectiveness of the MC for DTAC applications, the damage is simulated in the structure through changes in its mass and stiffness values, causing natural frequency shift and changes in damping of the structure modes. For this purpose, four configurations are induced sequentially to simulate damage severity increase:

1. Healthy: no changes in mass or stiffness (reference model).
2. Damage 1: reduction in masses m_2 and m_3 of 10% relative to the reference model.
3. Damage 2: reduction in stiffness coefficients k_1 and k_4 of 10% relative to configuration 2.
4. Damage 3: reduction in stiffness coefficients k_2 and k_3 of 20% relative to configuration 3.

The MC and the RC designed for the healthy structure are examined for DTAC using the models of configurations 2–4. The performance comparison between the RC and the MC is presented in Fig. 4. For all configurations, the MC is more effective in vibration reduction than the RC, as can be noted by analyzing the frequency responses presented in Fig. 4a and b. These results show that an appropriate vibration reduction in each mode decreases damage effects in the controlled system performance. However, this performance increase generally implies an increase in the control effort, as can be seen in Fig. 4c.

4.2. Experimental results

The experimental setup consists of two similar aluminum beams of 700 mm with cantilever boundary conditions and rectangular cross sections of 3.2 mm×32 mm. In each side of the beams, a PZT element with dimensions of 0.3 mm×20 mm×30 mm is glued 50 mm away from the origin and is used as an actuator. To apply the disturbance signal, PZTs with dimensions of 0.2 mm×20 mm×30 mm are glued to both sides of the beams 120 mm far from the origin. As a sensor, a PZT with dimensions of 0.5 mm×20 mm×20 mm is glued 110 mm away from the end on one side of each beam. The beams are presented in Fig. 5a. The block diagram used to illustrate the experimental configuration for DTAC purpose is shown in Fig. 5b. Furthermore, the dotted triangular prism represents completely removed material to act as the induced damage. The signal generation, data acquisition, and the controller are implemented using a dSPACE® board, model DS1104, and ControlDesk® software. The control signal $u(t)$ and disturbance signal $w(t)$ are generated and amplified 20 times and are applied to their respective transducers. The vibration signal $y(t)$ is captured by a PZT sensor, then it is conditioned and transmitted to the acquisition.

4.2.1. Healthy structure identification

The experimental frequency responses (EFRs) are estimated using the deterministic Schroeder signal as excitation, sampled at 4 kHz and with frequency band between 0 Hz and 500 Hz. An EFR can be written as (Pintelon & Schoukens, 2001):

$$P_{ba} = \frac{S_{ba}}{S_{aa}},$$

in which $a(t)$ represents the input signal ($u(t)$ or $w(t)$), and $b(t)$ is the output signal ($y(t)$). S_{aa} is the power spectral density of $a(t)$, and S_{ba} is the cross power spectral density between $b(t)$ and $a(t)$.

To determine P_{yu}, the Schroeder signal is applied to the piezoelectric actuator and the disturbance signal is set to zero. Similarly, P_{yw} is determined when the Schroeder signal is considered as disturbance and the signal $u(t)$ is set to zero. Furthermore, forty periods of the Schroeder signal are used to estimate each EFR. The experimental estimation of P_{yu} and P_{yw} is presented in Fig. 6. One may note that P_{yu} and P_{yw} show five different modes. However, the first peak of P_{yw} is much smaller than the other four peaks. Thus, as the objective is to reduce the structure vibrations when there is some disturbance, the first mode can be ignored in the identification. Therefore, using the *ssest* function of MATLAB®, the structure model is identified in the state-space modal representation as a multiple-input-single-output system considering four main modes of vibration. The identification results can be compared with the EFRs in Fig. 6.

4.2.2. Modal robust controller design

The control design criterion here adopted is to suppress vibration in the first three recognized modes of the flexible beam subject to damage. Thus, the modal model is truncated including only the first three modes, as can be seen in Fig. 7. The lost information in the reduced model may affect dynamics and bring undesirable effects such as spillover. To avoid this effect, both weighing functions of (12) are designed with the following parameters: M=255, k=1, $\varepsilon = 0.1$, and $w_c = 1800$ rad/s.

The plant model is built in the state-space form with matrices

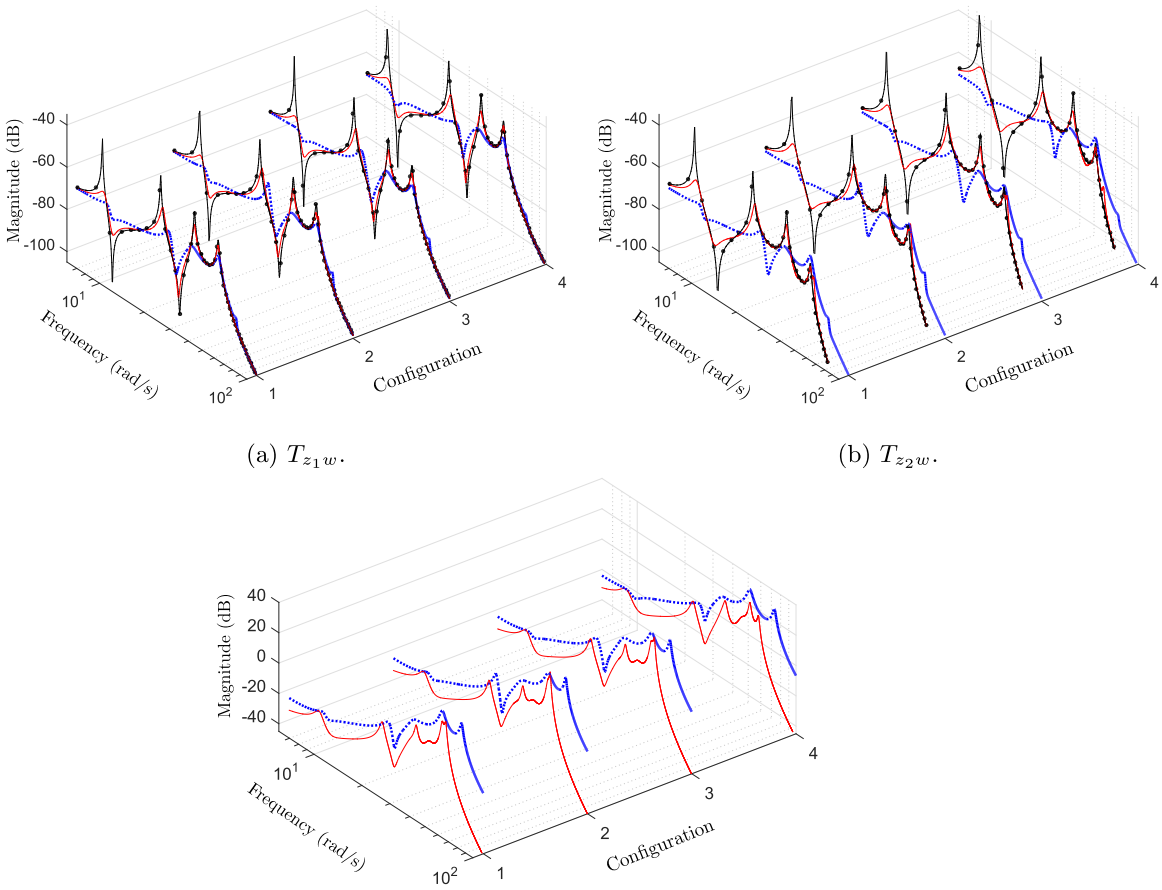

(a) $T_{z_1 w}$.

(b) $T_{z_2 w}$.

(c) T_{uw}.

Fig. 4. Performance comparison between open loop (black line with points), RC (red solid line), and MC (blue dotted line) for the simulated structure. (For interpretation of the references to color in this figure legend, the reader is referred to the web version of this article).

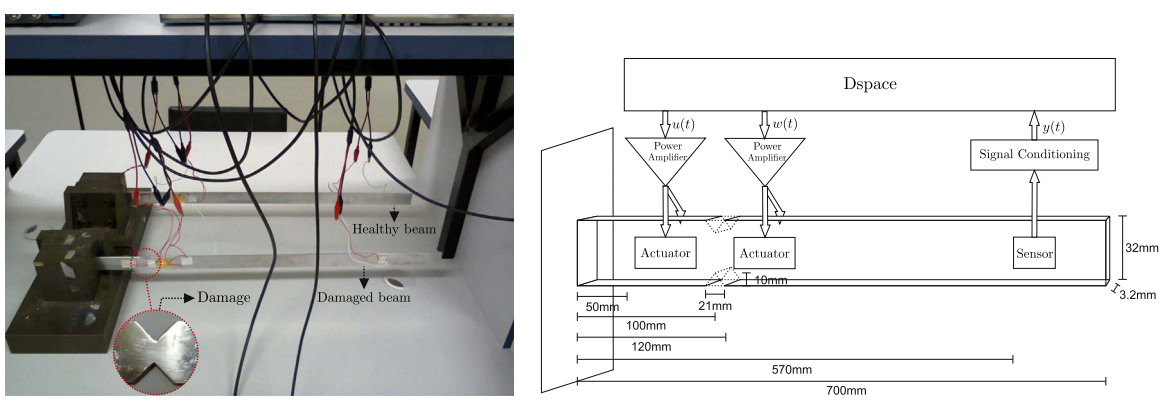

(a) Aluminum beams.

(b) Block diagram.

Fig. 5. Experiment setup.

($\mathbf{A}$, $\mathbf{B_1}$, $\mathbf{B_2}$, $\mathbf{C_2}$, $\mathbf{D_{21}}$, $\mathbf{D_{22}}$) obtained directly from truncation of the identified model, whose performance matrices are adopted as $\mathbf{C_1} = \mathbf{C_2}$ and $\mathbf{D_{11}} = \mathbf{D_{12}} = 0$. In the simulations and experiments, a chirp signal with band between 78 Hz and 500 Hz, duration of 5.4 s, and amplitude of 0.5 V is considered as disturbance.

The RC is initially designed and its performance is used as the reference. The RC reduces the vibration level over the four modes, three modes in the interest band and another out, as can be seen in Fig. 8. To analyze the weighing effects in the modes, three configurations are created:

1. MC1: $[\mathbf{Q_1}^{1/2}\ \mathbf{Q_2}^{1/2}\ \mathbf{Q_3}^{1/2}] = [0.5\ 1.0\ 1.2]$;
2. MC2: $[\mathbf{Q_1}^{1/2}\ \mathbf{Q_2}^{1/2}\ \mathbf{Q_3}^{1/2}] = [0.5\ 1.2\ 1.4]$;
3. MC3: $[\mathbf{Q_1}^{1/2}\ \mathbf{Q_2}^{1/2}\ \mathbf{Q_3}^{1/2}] = [0.5\ 1.4\ 1.6]$.

Fig. 8a shows modal peak vibration of the healthy structure. The modal vibration reduction is optimized by increasing the mode weighing. Also, the MCs are more effective in reducing vibration than

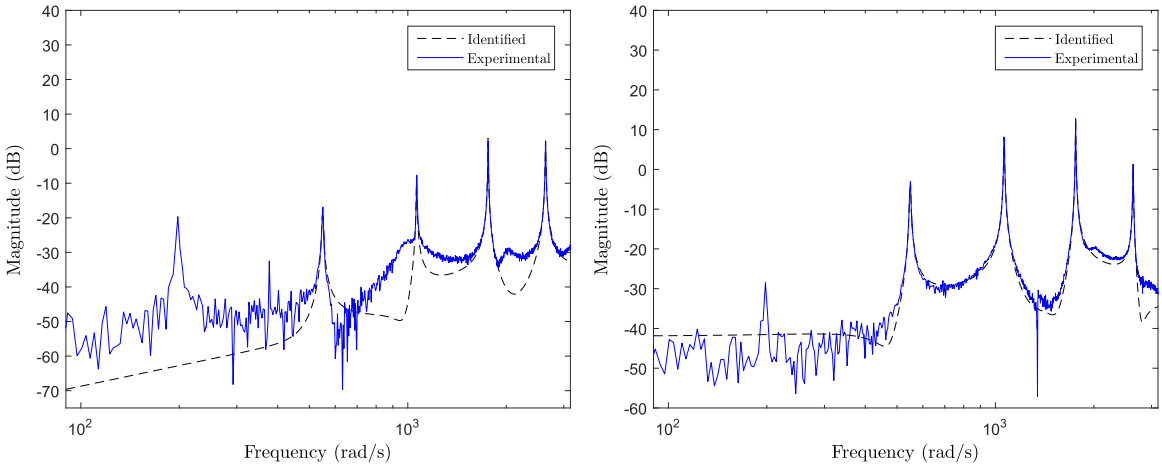

(a) P_{yu}. (b) P_{yw}.

Fig. 6. Experimental and identified P_{yu} and P_{yw}.

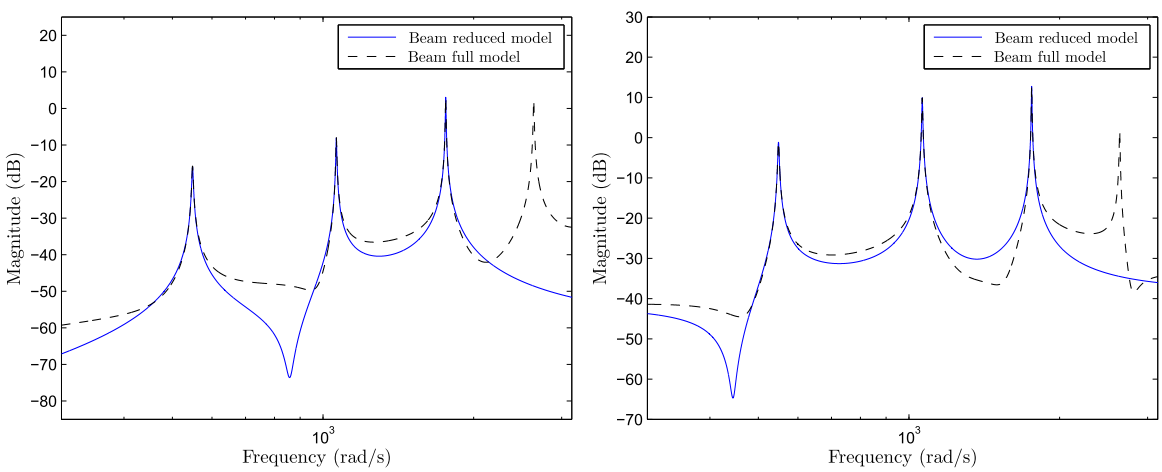

(a) Transfer functions between $y(t)$ and $u(t)$. (b) Transfer functions between $y(t)$ and $w(t)$.

Fig. 7. Transfer function comparison between full and reduced models.

the RC. These results are demonstrated more clearly by analyzing the percentage reduction in Fig. 8b, computed in relation to the open-loop response of the healthy structure. Moreover, the control signal amplitude increases with mode weights, as can be seen in Fig. 8c.

4.2.3. Control system experimental application

To test the modal H_∞ control methodology for regular vibration control and for DTAC purpose, the controllers designed for the healthy beam are experimentally examined in the healthy beam and in the damaged beam. Fig. 9 shows the open-loop frequency response comparison of the healthy and the damaged structures. It is possible to notice that damage produces natural frequency shifts in all modes. Damage also provokes amplitude increase in almost all modes, decreasing only in the last mode of P_{yw}, which is outside the interest band.

The experimental data analysis starts with the healthy beam experimental vibration signals, whose peak vibration of each mode is shown in Fig. 10a. The relative vibration reduction is presented in Fig. 10b, adopting the open-loop response of the healthy structure as the reference. Similarly to the simulated case, the RC reduces the global vibration in the interest band. For MCs, the vibration reduction in each mode is enhanced by the increasing mode weight. For instance, the third mode weight is continuously increased and its vibration is continuously reduced. For mode 1, the RC is causing the greatest vibration reduction. This result is expected because the MCs have a low weight in this mode. For mode 2, the MC1 does not change its weight, so it has a response similar to the regular H_∞ controller. For mode 4, which is outside the interest band, the amplitude is attenuated in relation to the open-loop response, considering all tested controllers. Analogously to the simulated results, the weighing increases the experimental control signal as can be seen in Fig. 11a.

The peak vibration and the relative vibration reduction of the damaged structure are shown respectively in Fig. 10a and b, adopting the open-loop response of the damaged structure as the reference to compute the percentage of vibration reduction. Damage increases vibration mode amplitudes in the interest bandwidth. However, all controllers showed to be effective in reducing vibrations. The modal controllers continue to present superior performance in relation to the RC, but this performance difference between the MCs and the RC is increased when compared with results of the healthy beam. Moreover, the MC3 reduces substantially mode 3 peak vibration in the damaged beam, reaching similar values of the best results of the closed-loop healthy beam. Mode 2 has a slighter performance because this mode is less weighted. For mode 4, which is outside the interest band, the attenuation is more effective for the damaged beam, considering that damage itself provokes vibration attenuation of this mode. However, the percentage reduction is similar for the healthy and the damage structures. Fig. 11b shows that the weight increase also implies a rise in

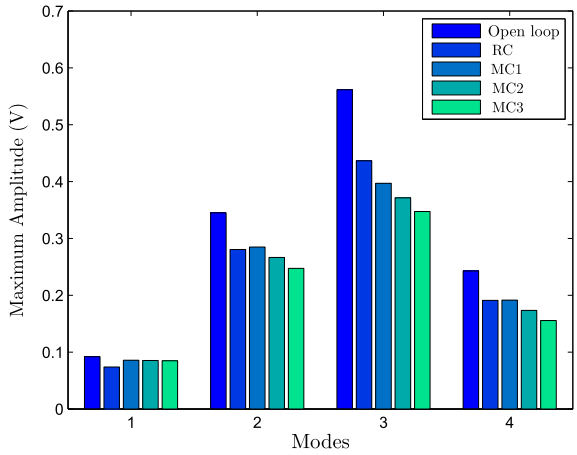

(a) Peak vibration of each mode.

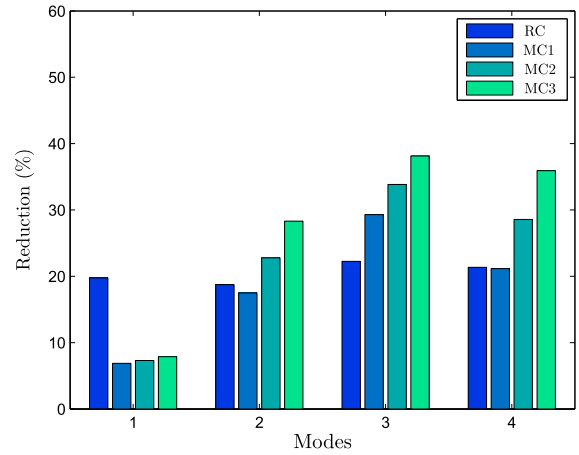

(b) Percentage reduction.

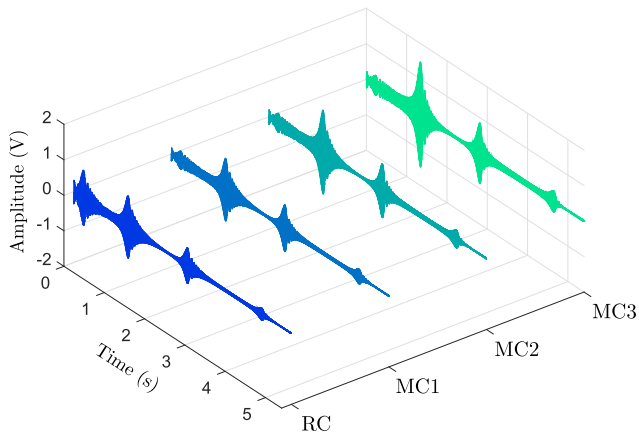

(c) Control signals.

Fig. 8. Healthy beam simulated signals.

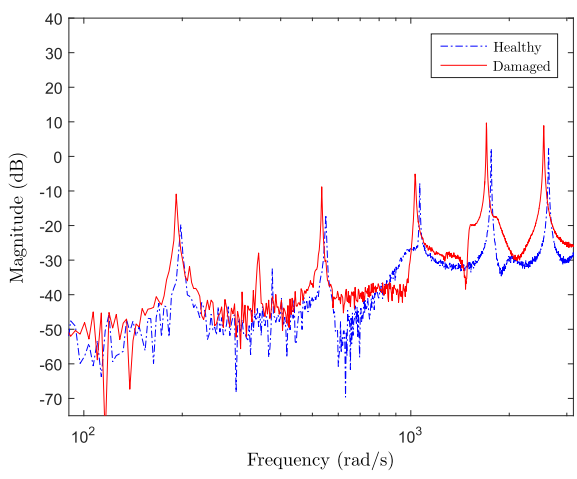

(a) P_{yu}.

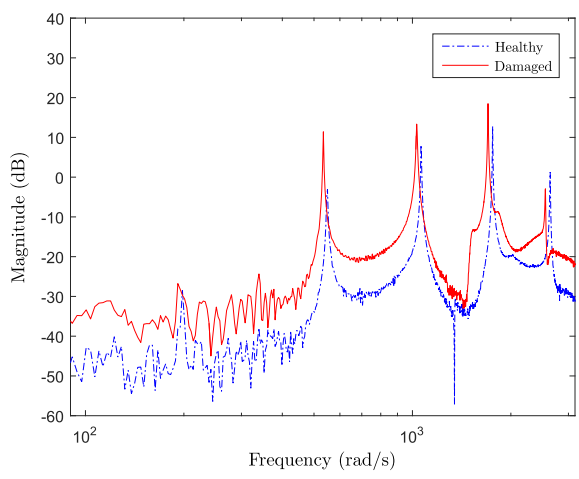

(b) P_{yw}.

Fig. 9. Frequency response comparison between healthy and damaged structures.

the control signal. As a final analysis, these experimental results show that an adequate control of the selected modes produces better results than the RC when the structure undergoes damage.

5. Conclusion

DTAC is a new research area targeting to adapt fault-tolerant control concepts to mechanical structures submitted to damage. In this paper, a novel modal H_∞ control methodology is presented and its capability of being applied to DTAC is shown through simulated and experimental examples. The proposed modal H_∞ approach provides control energy distribution over selected modes, which is appropriate to reduce damage effects. A weighed modal H_∞ norm is introduced, where the modal weighing leads to the high modal selectivity property,

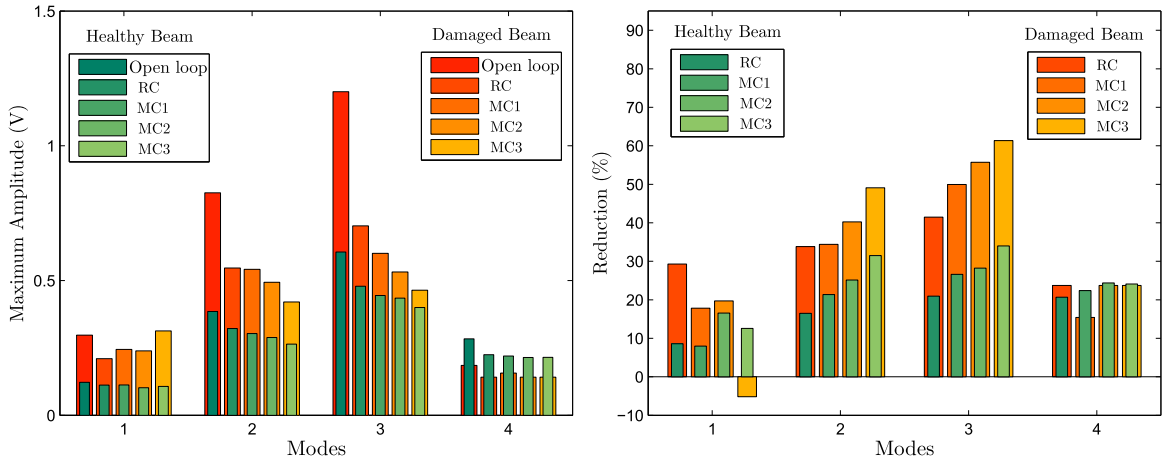

(a) Peak vibration of each mode. (b) Percentage reduction.

Fig. 10. Experimental output signals.

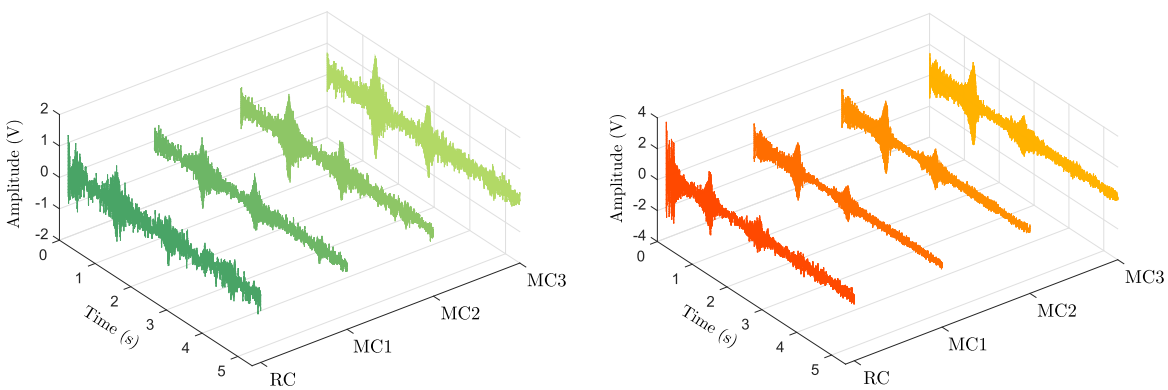

(a) Healthy beam. (b) Damaged beam.

Fig. 11. Experimental control signals.

which permits to design efficient and robust modal controllers. The methodology effectiveness was examined through applications with different levels of difficulty. Initially, the proposed design approach is applied to a simulated system with four masses connected by springs and dampers, and damage is included by changes in the respective parameters. Then, the methodology is experimentally tested using two similar cantilever aluminum beams, in which damage is introduced by material removal. Results show that the modal H_∞ approach is more effective than the regular H_∞ technique in mitigating structural vibration in the analyzed cases, opening up the possibility of modal selectivity and effective control including damage tolerance. As future work objective, an adaptive law will be used to update the weighing matrices online, considering the damage impact in each mode. For this purpose, a damage detection and assessment technique will be integrated into the modal H_∞ control methodology.

Acknowledgements

The author Helói F. G. Genari gratefully acknowledges the financial support received from CNPq (“Bolsista CNPq – Proc. no 141621/2012-5”) and CAPES (“Bolsista da CAPES – Proc. no 12337/13-7”).

References

Balas, M. J. (1978). Active control of flexible systems. *Journal of Optimization Theory and Applications*, *25*(3), 415–436.

Balas, M. J. (1979). Direct velocity feedback control of large space structures. *Journal of Guidance, Control, and Dynamics*, *2*(3), 252–253.

Baz, A., & Poh, S. (1990). Experimental implementation of the modified independent modal space control method. *Journal of Sound and Vibration*, *139*(1), 133–149.

Bossi, L., Rottenbacher, C., Mimmi, G., & Magni, L. (2011). Multivariable predictive control for vibrating structures: An application. *Control Engineering Practice*, *19*(10), 1087–1098.

Boulet, B., Francis, B. A., Hughes, P. C., & Hong, T. (2001). μ synthesis for a large flexible space structure experimental testbed. *Journal of Guidance, Control, and Dynamics*, *24*(5), 967–977.

Braghin, F., Cinquemani, S., & Resta, F. (2012). A new approach to the synthesis of modal control laws in active structural vibration control. *Journal of Vibration and Control*, 1–20.

Chilali, M., & Gahinet, P. (1996). H_∞ design with pole placement constraints: an LMI approach. *IEEE Transactions on Automatic Control*, *41*(3), 358–367.

Chomette, B., Rémond, D., Chesné, S., & Gaudiller, L. (2008). Semi-adaptive modal control of on-board electronic boards using an identification method. *Smart Materials and Structures*, *17*(6), 1–8.

Chomette, B., Chesné, S., Rémond, D., & Gaudiller, L. (2010). Damage reduction of on-board structures using piezoelectric components and active modal control: application to a printed circuit board. *Mechanical Systems and Signal Processing*, *24*(2), 352–364.

Cinquemani, S., Ferrari, D., & Bayati, I. (2015). Reduction of spillover effects on independent modal space control through optimal placement of sensors and actuators. *Smart Materials and Structures*, *24*(8), 1–11.

Fang, J. Q., Li, Q. S., & Jeary, A. P. (2003). Modified independent modal space control of m.d.o.f. systems. *Journal of Sound and Vibration*, *261*(3), 421–441.

Gahinet, P., & Apkarian, P. (1994). A linear matrix inequality approach to H_∞ control. *International Journal of Robust and Nonlinear Control*, *4*(4), 421–448.

Gahinet, P., Nemirovski, A., Laub, A. J., & Chilali, M. (1995). *LMI control toolbox: for use with MATLAB®*. The MathWorks.

Gawronski, W. (2004). *Advanced structural dynamics and active control of structures*. Springer-Verlag.

Gawronski, W. (2008). *Modeling and control of antennas and telescopes*. Springer.

Genari, H. F. G., Oliveira Neto, O., Nóbrega, E. G. O., Mechbal, N., & Coffignal, G., (2015). Robust vibration control of a vertical flexible structure subject to seismic

events. In *XVII international symposium on dynamic problems of mechanics – DINAME 2015* (pp. 1–10). Natal, Brazil.

Genari, H. F. G., Mechbal, N., Coffignal, G., & Nóbrega, E. G. O. (2015). A modal H_∞ control methodology for damage-tolerant active control. In *Proceedings of the 9th IFAC symposium on fault detection, supervision and safety for technical processes* (pp. 664–669). Paris, France.

Gosiewski, Z., & Kulesza, Z. (2013). Virtual collocation of sensors and actuators for a flexible rotor supported by active magnetic bearings. In *Proceedings of the 14th international carpathian control conference* (pp. 94–99). Rytro.

Gu, H., & Song, G. (2005). Active vibration suppression of a composite I-beam using fuzzy positive position control. *Smart Materials and Structures*, *14*(4), 540–547.

Halim, D. (2004). Control of flexible structures with spatially varying disturbance: Spatial H_∞ approach. In *Proceedings of the 43rd IEEE conference on decision and control* (vol. 5, pp. 5065–5070). Atlantis, Paradise Island, Bahamas.

Hu, Y.-R., & Ng, A. (2005). Active robust vibration control of flexible structures. *Journal of Sound and Vibration*, *288*(1–2), 43–56.

Inman, D. J. (1989). *Vibration with control, measurement, and stability*. Prentice-Hall Internation Editions.

Inman, D. J. (2001). Active modal control for smart structures. *Philosophical Transactions of the Royal Society A*, *359*, 205–219.

Khot, S., Yelve, N. P., Tomar, R., Desai, S., & Vittal, S. (2011). Active vibration control of cantilever beam by using PID based output feedback controller. *Journal of Vibration and Control*, *18*(3), 366–372.

Kim, S.-M., & Oh, J.-E. (2013). A modal filter approach to non-collocated vibration control of structures. *Journal of Sound and Vibration*, *332*(9), 2207–2221.

Kim, S.-M., Wang, S., & Brennan, M. J. (2011). Comparison of negative and positive position feedback control of a flexible structure. *Smart Materials and Structures*, *20*(1), 1–10.

Marinaki, M., Marinakis, Y., & Stavroulakis, G. E. (2010). Fuzzy control optimized by PSO for vibration suppression of beams. *Control Engineering Practice*, *18*(6), 618–629.

Mastory, C. G., & Chalhoub, N. G. (2014). Enhanced structural controllers for non-collocated systems. *Journal of Vibration and Control*, 1–17.

Mechbal, N., & Nóbrega, E. G. O. (2015). Spatial H_∞ approach to damage-tolerant active control. *Structural Control and Health Monitoring*, *22*(9), 1148–1172.

Mechbal, N., Vergé, M., Coffignal, G., & Ganapathi, M. (2006). Application of a combined active control and fault detection scheme to an active composite flexible structure. *Mechatronics*, *16*(3–4), 193–208.

Mechbal, N., & Nóbrega, E. G. O. (2012). Damage tolerant active control: Concept and state of the art. In *Proceedings of the 8th IFAC symposium on fault detection, supervision and safety of technical processes* (pp. 63–71). Mexico City, Mexico.

Mechbal, N., & Nóbrega, E. G. O. (2015a). Adaptive strategy to damage tolerant active control. In *Proceedings of the 9th IFAC symposium on fault detection, supervision and safety for technical processes* (pp. 658–663). Paris, France.

Meirovitch, L., & Baruh, H. (1985). The implementation of modal filters for control of structures. *Journal of Guidance, Control, and Dynamics*, *8*(6), 707–716.

Meirovitch, L., Baruh, H., & Oz, H. (1983). A comparison of control techniques for large flexible systems. *Journal of Guidance, Control, and Dynamics*, *6*(4), 302–310.

Mohamed, Z., Martins, J. M., Tokhi, M. O., Sá da Costa, J., & Botto, M. A. (2005). Vibration control of a very flexible manipulator system. *Control Engineering Practice*, *13*(3), 267–277.

Nesterov, Y., & Nemirovski, A. (1994). *Inteiror-point polynomial algorithms in convex programming*. SIAM Studies in Applied Theory Mathematics.

Nonami, K., & Sivrioglu, S. (1996). Active vibration control using LMI-based mixed H_2/H_∞ state and output feedback control with nonlinearity. In *Proceedings of the 35th IEEE conference on decision and control* (vol. 1, pp. 161–166). Kobe.

Pereira, E., Aphale, S. S., Feliu, V., & Moheimani, S. O. R. (2011). Integral resonant control for vibration damping and precise tip-positioning of a single-link flexible manipulator. *IEEE/ASME Transactions on Mechatronics*, *16*(2), 232–240.

Petersen, I. R., & Pota, H. R. (2003). Minimax LQG optimal control of a flexible beam. *Control Engineering Practice*, *11*(11), 1273–1287.

Pintelon, R., & Schoukens, J. (2001). *System identification: A frequency domain approach*. IEEE Press.

Preumont, A. (2011). *Vibration control of active structures: An introduction* (3rd ed.). Springer.

Resta, F., Ripamonti, F., Cazzulani, G., & Ferrari, M. (2010). Independent modal control for nonlinear flexible structures: An experimental test rig. *Journal of Sound and Vibration*, *329*(8), 961–972.

Robu, B., Budinger, V., Baudouin, L., Prieur, C., & Arzelier, D. (2010). Simultaneous H_∞ vibration control of fluid/plate system via reduced-order controller. In *Proceedings of the 49th IEEE conference on decision and control* (pp. 3146–3151). Atlanta, GA.

Schröck, J., Meurer, T., & Kugi, A. (2011). Non-collocated feedback stabilization of a non-uniform Euler-Bernoulli beam with in-domain actuation. In *Proceedings of the 50th IEEE conference on decision and control and european control conference* (pp. 2776–2781). Orlando, FL.

Serpa, A. L., & Nobrega, E. G. O. (2005). H_∞ control with pole placement constraints for flexible structures vibration reduction. In *18th international congress of mechanical engineering – COBEM2005* (pp. 1–8). Ouro Preto, Brazil.

Serra, M., Resta, F., & Ripamonti, F. (2013). Dependent modal space control. *Smart Materials and Structures*, *22*(10), 1–11.

Tang, X., & Chen, I. (2009). Robust control of XYZ flexure-based micromanipulator with large motion. *Frontiers of Mechanical Engineering in China*, *4*(1), 25–34.

Zabihollah, A., Sedagahti, R., & Ganesan, R. (2007). Active vibration suppression of smart laminated beams using layerwise theory and an optimal control strategy. *Smart Materials and Structures*, *16*(6), 2190–2201.

Zhang, J., He, L., Wang, E., & Gao, R. (2009). Robust active vibration control of flexible structures based on H_∞ control theorem. In *International workshop on intelligent systems and applications* (pp. 1–6). Wuhan.

Zhou, K., & Doyle, J. C. (1997). *Essentials of robust control*. Prentice Hall.